Towards a Neural Co-Processor Which Restores Dexterity After Stroke: Modeling a Proof-of-Concept

Matthew J Bryan[1], **Linxing Preston Jiang**[1], **Rajesh P N Rao**[1]

[1] Neural Systems Laboratory, Department of Computer Science and Engineering, University of Washington, Box 352350, Seattle, WA 98105, USA

E-mail: matthew.bryan@dell.com

September 2021

Abstract. *Objective* Brain co-processors [1] are devices which use artificial intelligence (AI) for closed-loop neurostimulation, to shape neural activity and to bridge injured neural circuits for targeted repair and rehabilitation. The co-processor framework offers a flexible approach to learning closed-loop stimulation policies that optimize for (a) specific regimes of neural activity, or (b) external task performance. For example, one may seek to learn to stimulate the motor cortex of a stroke patient, conditioning the stimulation on upstream visual information, aiding the patient's attempt to grasp an object. Through the use of artificial neural networks (ANNs) and deep learning, the co-processor co-adapts with the neural circuit, allowing it to seek optimal stimulation policies, and adapt them as the neural circuit changes. The results presented here demonstrate a neural co-processor for the first time, through the use of a simulation. We explore some of the core algorithms that may allow co-processors to successfully learn, and to adapt to non-stationarity in both the brain and sensors. *Approach* We provide the first proof-of-concept of a neural co-processor that leverages deep learning, through the use of a simulated neural circuit. That circuit performs a reach-to-grasp task, based on visual input, and is designed to closely resemble a similar circuit in a primate brain [2]. We simulate a variety of lesions by altering the model, and then demonstrate our co-processor's ability to restore lost function through "stimulation" of that model. We further test the ability of our co-processor to adapt its stimulation as the simulated brain undergoes changes. *Main results* Our simulated co-processor successfully co-adapts with the neural circuit to accomplish the external reaching task. The co-processor framework demonstrated here adapts to a variety of lesion types, and to ongoing changes in the simulated brain. *Significance* The proof-of-concept here outlines a co-processor model, as well as our approach to training it, leading to insights on how such a model may be developed for *in vivo* use. We believe this co-processor design has potential to learn complex stimulation policies, leading to application in treating a variety of diseases.

Keywords: brain-computer interface, neural co-processor, ai, machine learning, stimulation

1. Introduction

Aided in part by application of advanced AI techniques, brain-computer interfaces (BCIs) have made advancements over the last several decades, allowing for decoded brain signals to be used for control of a wide variety of virtual and physical prostheses [3, 4, 5, 6]. Separately: advances in stimulation techniques and modeling have allowed us to probe neural circuit dynamics (e.g. [7]) and learn to better drive neural circuits towards target dynamics, by encoding and delivering information through stimulation [8, 9, 10, 11, 12, 13, 14, 15]. Recently, there has been increasing interest in building on these advances to combine decoding and encoding in a single system, for closed-loop stimulation of a neural circuit. Bi-directional BCIs (BBCIs) allow stimulation to be conditioned by decoded brain activity as well as external sensor (e.g. camera) data, which can allow for the application of real-time, fine-grained control of neural circuits and prosthetic devices, e.g. Nicolelis et al. [16]. These may lead, for example, to neuro-prostheses that are capable of restoring movement which was lost due to traumatic brain injury (TBI), to a degree not previously possible.

Motivated by that progress, we demonstrate here a flexible framework for combining encoding and decoding, which we term "neural co-processors" [1]. Neural co-processors leverage AI and deep learning to identify optimal, closed-loop stimulation patterns. The approach is flexible enough to optimize not only for particular neural activities, but also for tasks external to the subject. For example, they may be able to aid a stroke patient by finding a stimulation pattern of the motor cortex which helps restore lost limb function. Likewise, the framework generalizes enough to condition stimulation on both brain activity, and external sensors, e.g. cameras or light detection and ranging (LIDAR) sensors, in order to incorporate feedback for realtime control.

Additionally, the co-processor framework allows a neuro-prosthesis to actively adapt to a neural circuit as it changes with time. This framework is capable of co-adapting with the circuit, i.e. brain, by updating its stimulation regime, while at the same time the brain is updating its response to the stimulation, and changing due to natural plasticity and aging. This allows the co-processor to continually optimize for the intended cost function, despite the signficant non-stationarity of the target circuit.

Here we provide a proof-of-concept in simulation for a co-processor that restores movement to a limb, after a subject has suffered a stroke affecting their ability to use that limb. It combines:

- A stimulation model, which models the relationship between decoded brain activity, stimulation, and task performance.
- An AI agent which determines the stimulation to apply in a closed-loop fashion, in real time.

2. Background

Significant advances have been made in modeling the effects of electrical stimulation of the brain, some of which can be leveraged for our co-processor design, as we outline below. Researchers have explored how information can be biomimetically or artificially encoded and delivered via stimulation to neuronal networks in the brain and other regions of the nervous system for auditory [8], visual [9], proprioceptive [10], and tactile [11, 12, 13, 14, 15] perception. Advancements have also been made in modeling the effects of stimulation over large scale, multi-region networks, and across time [17]. Some have additionally designed models which can adapt to ongoing changes in the brain, including changes due to the stimulation itself [18]. In our proof-of-concept outlined below, we will use a stimulation model, not unlike those cited here, which seeks to account for both network dynamics and non-stationarity. In addition to training the model to have a strong ability to predict the effect of stimulation, we additionally train it to be useful for then learning an optimal stimulation policy, which we will show is a property somewhat distinct from predictive power alone.

Advances have also been made in both open- and closed-loop stimulation for treating a variety of disorders. Open loop stimulation has been effective in treating Parkinson's Disease (PD) [19], as well as various psychiatric disorders [20, 21, 22]. More directly related to this paper, we see in Khanna et al. [23], the use of open loop stimulation in restoring dexterity after a lesion of a primate's motor cortex. The authors demonstrate that the use of low-frequency alternating current, applied epidurally, can improve grasp performance.

While open loop stimulation techniques have yielded clinically useful results, their results in many domains have been mixed, such as use in visual prostheses [24], and use in invoking somatosensory feedback [15]. Likely this is due to the stimulation not being conditioned on the ongoing dynamics of the circuit being stimulated. Moment-to-moment and throughout the day, the circuit will respond differently to the same stimulus, as a result of differing inputs and ongoing activity. Stimulation therefore needs to be proactively adapted in response [17, 25]. This need is even greater over longer time scales as the effects of plasticity and ageing change the connectivity of the brain. Closed-loop stimulation may also provide means to better regulate the energy use of an implanted stimulator, allowing it to intelligently regulate when to apply stimulation, in order to preserve implant battery life. Closed-loop stimulation also offers an opportunity minimize side-effects of stimulation, through real time regulation of the stimulation parameters, such as in the use of deep brain stimulation (DBS) in PD patients [26].

Closed-loop stimulation conditions stimulation on observations of brain activity, allowing it to shape the neural activity more precisely, and in response to changes in a patient's clinical condition. This may also allow an implant to adapt in real time to changes in the target circuit. It has been used to aid in learning new memories after some impairment [27, 28], to replay visually-invoked activations [18], and for optogenetic control of a thalamocortical circuit [29], among others.

Something that remains unclear is how to leverage closed-loop control for real-time co-adaption with the brain to accomplish an external task. "Co-adaption" here refers to the ability of a neuro-prosthesis to adapt its stimulation regime to the ongoing changes in the circuit it is stimulating, and to adapt with that circuit to accomplish the external task, such as grasping. The neural co-processor we present here provides one potential model for accomplishing that. Through the use of deep learning, the co-processor model we present co-adapts an AI agent, which governs the stimulation, with both a stimulation model, and the neural circuit being stimulated.

For a neurologically complex task such as grasping, we cannot identify *a priori* a real time stimulation regime of the neural circuit which would result in precise task-relevant control. That is due in large part to the variability of circuits from subject-to-subject, as well as variations in the placement of sensors and stimulators in the brain. The only plausible path to such a real time controller is to parameterize it in a subject- and time-specific way. Our model seeks to accomplish that using deep learning.

Before attempting *in vivo* experiments using such a model, we first demonstrate here a number of crucial design elements of it, through the use of a simulated grasping circuit, presented previously by Michaels et al. [2]. We explore the properties of the co-processor design that are needed to successfully adapt to the long-running dynamics of a stimulated neural circuit, as well as to adapt to that circuit's ongoing connectivity changes. We additionally present a training method for our co-processor, allowing it to learn an optimal stimulation pattern that drives improvements in external task performance, while also adapting to the non-stationarity of the brain.

3. Method

3.1. Architecture Overview

First, we present the architecture of our co-processor design. This design aims to solve two fundamental challenges in using neural stimulation to improve external task performance. First, neural networks exhibit long-running and nonlinear dynamics, necessitating the need for a stimulation agent to account for far-distant effects of the stimulation it applies. Second, with neurologically complex tasks, such as grasping, the mapping between neural activity as-measured and the external task cannot be determined *a priori*. As a result, the co-processor must somehow learn what stimulation is appropriate for aiding the user in the external task they are attempting to perform.

Our co-processor attempts to solve these with a pair of artificial neural networks:

- A stimulation and neural dynamics model, known as an "Emulator Network" (EN). It models the relationship between the stimulation, neural dynamics, and external task. Its purpose is for training the second network, by accurately modeling the effect of stimulation.
- A stimulation agent, known as the "co-processor network" (CPN), which maps neural activity, and possibly data from external sensors, to stimulation parameters.

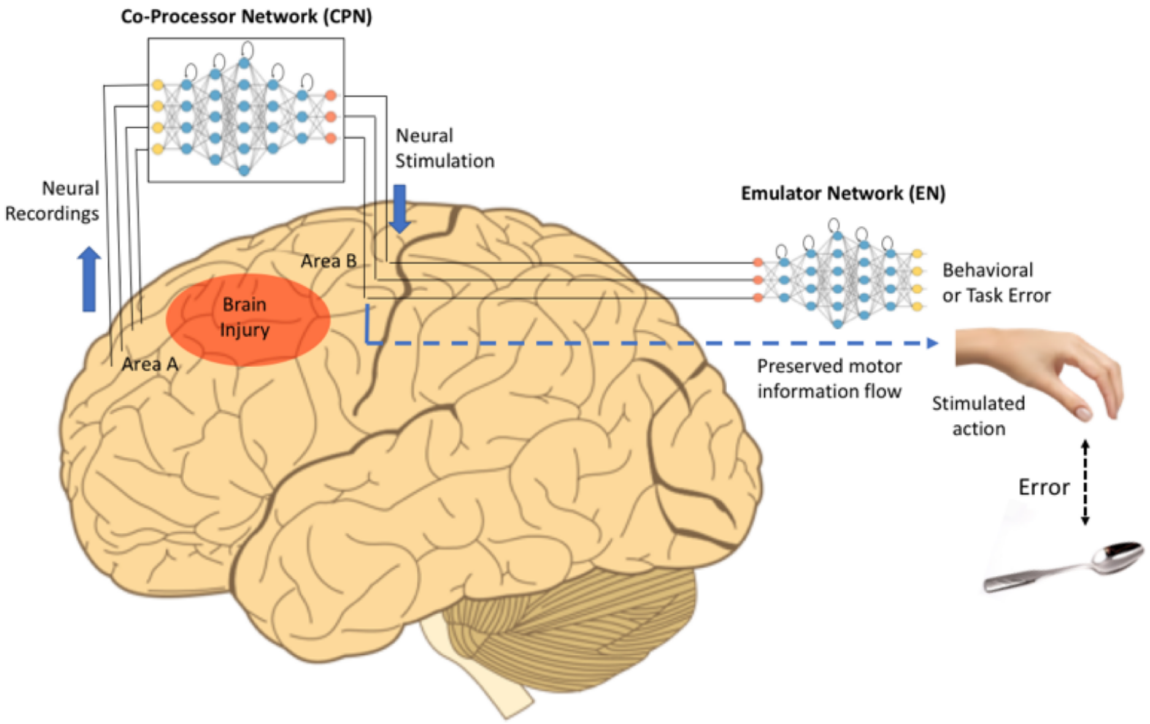

Figure 1: Using a co-processor to drive external task performance after a traumatic brain injury

We co-train the EN and CPN, with the goal of training a CPN whose output stimulation parameters improve task performance. By iteratively training and retraining both over time, they adapt to the brain as it changes, effectively allowing for brain-stimulator co-adaptation. The EN is a tool for training the CPN, giving us a way to backpropagate task error to the CPN. It outputs task-relevant metrics - a prediction of muscle velocities in our case - given measurements of neural activity, and the stimulation parameters output from the CPN. If the EN is trained in a particular way, and to a sufficient level of precision, it can be used as a function approximator relating stimulation and a task, and do so in a way that allows us to train the CPN with it. When training the CPN, we in-effect treat the EN's output as the true value of the task-relevant metric, or a related metric, and then backpropagate the loss defined in terms of that metric in order to train the CPN. See Fig. 1. We will illustrate the details of the training algorithm below.

Put another way: we define our loss functions for both the EN and CPN based on an L2 error over a vector of muscle length velocities. The EN's error measures the EN's prediction error for some stimulation and measured neural activity. The CPN's error measures the difference between actual and target muscle length velocities. In our case, those targets come from the simulated task; see below.

In our present demonstration, the EN is constituted as a single layer, fully connected, long short-term memory (LSTM) recurrent neural network (RNN), with

hyperbolic tangent (*tanh*) activations, and a linear readout. The general notion of a co-processor does not require this precise architecture, but for our example, we found that the LSTM approach allows the network to continuously adapt to long-running dependencies in the simulated neural dynamics, far better than a vanilla RNN. The CPN is constituted as an almost identical network, though with a different dimensionality, as we explain below. There is no strict requirement for the EN and CPN to be so similar, but we found this simple architecture to work well in our example.

Note that the EN effectively constitutes a stimulation model. However, in the case that a co-processor attempts to optimize for task performance, as opposed to neural activity directly, the stimulation model predicts the effect of stimulation and neural dynamics on task performance, rather than modeling and predicting the neural response to stimulation alone. This provides the key functionality needed to train the CPN.

We initially attempted an EN architecture using vanilla RNN cells, with a nonlinearity. This approach resembles the common linear time-invariant state space model of stimulation, as in e.g. Yang et al. [17], though it additionally incorporates a nonlinearity. That approach has the benefit of being simple, and familiar. We found, however, that the linear approach, as well as the related vanilla RNN approach with nonlinearities added, was not sufficiently expressive of long-term dependencies, such that the co-processor was capable of learning well.

Separately, nonlinear LSTM models have also been applied to modeling natural neural networks, such as use in predicting local field potentials [30], and for stimulation modeling [31]. LSTM cells are designed to better capture the relevant aspects of long-running network dynamics. We found that LSTM cells were crucial for enabling our co-processor to learn the long-running dynamics of the network it was stimulating, and we use them as a result.

3.2. Simulation Overview

We demonstrate our approach here using a simulated grasping circuit. A detailed simulation such as this allows us to explore some of the critical architectural details and training algorithms that will allow a co-processor to succeed. By first doing such exploration in simulation, we are able to rapidly and cheaply iterate on our design, prior to any *in vivo* experiments. For the simulation to be admissible, we need to ensure it has some properties that allow it to strongly indicate if our design is improving in a direction that will later allow for real deployments. Otherwise, our design may be adapting to the pecularities of the simulation, without becoming more useful.

The simulated circuit, from Michaels et al. [2], was trained to resemble the grasping circuits of primate subjects engaged in a delayed reach-to-grasp task. Its design draws on a body of literature focused on architectures and training methods for RNNs which seek to create artificial neural circuits that have activation dynamics similar to natural circuits, including delayed grasping tasks [32]. The Michaels circuit consists of a "modular" vanilla RNN (mRNN), and a linear readout layer. Each "module" consists of

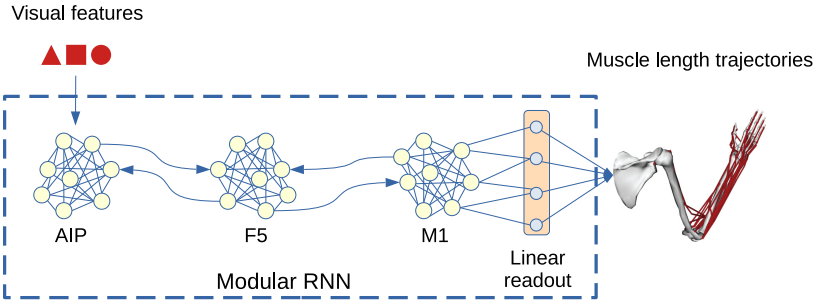

(a) Michaels Modular RNN (mRNN), a simulated grasping circuit [2]. The emergent dynamics of the three modules correspond well to natural neural activity measured from primate AIP, F5, M1 regions, respectively, from the same task. Visual (VGGNet) features forward propagate through the network, conditioning the grasp for the object of the particular size, shape, and location.

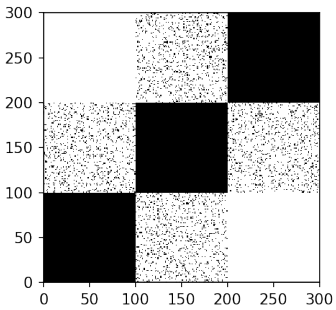

(b) Connectivity matrix J. Note the within-module connections (on the diagonal) are fully connected, and connections to adjacent modules are sparse 10%.

Figure 2: Architecture of the Michaels mRNN

100 vanilla RNN neurons, with a nonlinearity applied on the outputs. The modules are internally fully connected, and are connected to each other sparsely (10% connectivity). The inputs are visual features intended to capture the view the primates had during the task, specifically VGGNet features [33], from 3D renderings of the same objects which the primates grasped. The outputs are muscle length velocities for the shoulder, arm, and hand of the primate during the trial. The natural velocities were captured with a motion capturing glove, and the artificial neural network was trained to recapitulate those grasping motions. Data and trained models from this work were supplied to us by the lead author Jonathan Michaels, for the purpose of our present simulation. We re-implemented his model's logic in PyTorch, and loaded his trained parameters into it, for one of his subjects, arbitrarily chosen. See Fig. 2.

The design of the circuit is intended to resemble a vision-to-grasp pipeline, essentially representing the visual processing needed to reach the hand to the appropriate position for the grasp, and to form the hand properly for grasping the particular shape of object. The emergent dynamics of the artificial network's "modules", once trained, correspond roughly to the AIP, F5, and M1 portions of the primate subjects' brains. 'Correspond' here, notably, refers to the fact that the activity of the module receiving the visual inputs resembles the AIP activity of the primate subject from the same trials. Likewise, the second and third modules resemble the natural activity from the primate's F5 and M1 regions, respectively. The emergent network dynamics show a number of other correspondences to the primates' natural brain activity as well, as detailed in the paper. For convenience, we will refer to these modules throughout this paper using the brain region they correspond to.

Importantly, the simulated circuit's activity shows a relatively clear separation of the object shapes. That is - the visual information input to the network that

differentiates one trial from another is leveraged by the circuit to successfully condition the hand shape trajectory for grasping the object of that trial's particular shape, size, and location. The visual information forward-propagates through the network, through successive processing steps, where it is eventually leveraged to recapitulate the grasp appropriate for the object represented by the input visual features. It follows, then, that the classes are separable in some way by observing the distinct ways that the mRNN is activated by the classes' corresponding visual inputs. As we will note below: in the absense of this visual information forward propagating, the circuit can at-best learn a loss-minimizing grasp, stereotyped across all object sizes and shapes. Such a grasp bears some resemblance to all grasps the given primate performed, due to all trials being a reach-to-grasp preceded by a holding period, but performance suffers drastically.

Clearly, training and deploying a neural co-processor in a true brain involves challenges we don't capture with this simulation. This simulation does not constitute evidence that our method will, for example, immediately translate to true restoration of fine-grained control for individual fingers of a stroke patient. One clear challenge with doing so would be the sheer dimensionality of natural brain dynamics, and how that compares to the resolution of stimulation the co-processor can learn to apply. There exists a clear mismatch between the dimensionality of the underlying problem, sensor and stimulator technologies, and the amount of training data which can reasonably be collected to train a closed-loop neural controller. We argue that while this fact clearly creates a challenge for learning-based closed-loop stimulation, that nevertheless the insights we generate through this simulation are likely to be applicable. In the Discussion below, we will explore how those insights are likely to lead to initial demonstrations of the co-processor approach on lower dimensional problems. As we show next, the simulation exhibits a number of properties that reflect a real world application, which our co-processor design must contend with.

3.2.1. Simulated lesions cause real world failure modes Simulating a brain lesion in terms of this artificial network results in error modes that resemble a some natural lesions of a primate brain. For example, if we alter the network by zeroing the outputs of some of the first (input, or AIP) module's neurons, the reaching motion generally succeeds, but the finger muscle velocities show a high degree of error - effectively implying that the subject can somewhat reach to grasp, but cannot form a grasp appropriate for the object. That suggests that losing a portion of the cortical machinery needed to translate or forward-propagate object shape information to movement-related cortex can result in a reduced ability to pose the hand, though positioning of the hand may still roughly succeed. Muscle spasticity of the hand is also a common symptom of certain strokes in primates, and indeed many who suffer from them are still able to position their hand, even while being unable to form it properly for a grasp [23, 34]. In that sense, the error mode of this simulated lesion closely resembles natural stroke symptoms. However, the simulation is not intended to constitute a physical model of a lesion, i.e. to directly explain the connection between hand spasticity and the lesion.

If we instead "disconnect" communications between the F5 and M1 modules, we see a failure similar to the AIP lesion: movement is generally achieved, but we see a disproportionate impact on hand pose. Finally, if we lesion of a portion of the output module of the Michaels mRNN, roughly corresponding to M1, we see a more wholesale loss of movement, affecting even the ability to reach for the grasp. See Fig. 3 for examples.

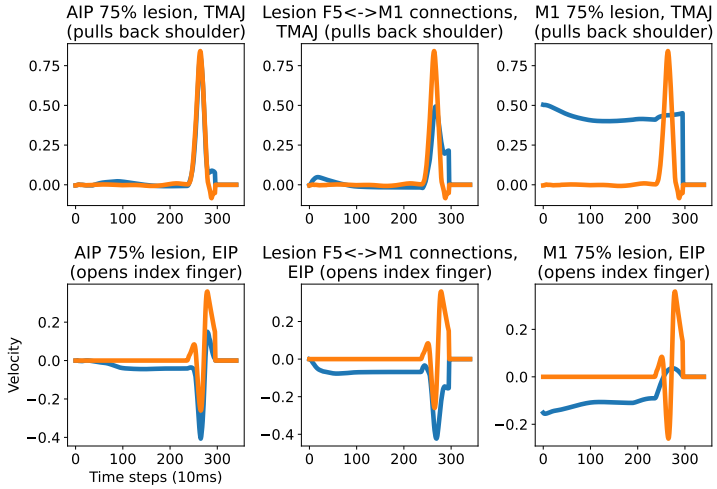

(a) Example muscle trajectories during a single trial, for one hand and shoulder muscle. Orange: original trajectory. Blue: with lesion.

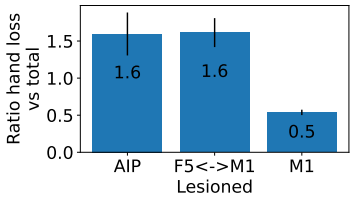

(b) Ratio of hand muscle MSE losses vs. overall MSE losses, for different lesion types. Average of all trials, with +/- 1 stdev shown.

Figure 3: Lesion designs which prevent forward propagation of object shape information differentially impact hand pose. Loss here is an L2 distance measured relative to the circuit's trajectories prior to the lesion.

The co-processor's task in our simulation will be identifying the appropriate information, read from the mRNN's activations, for conditioning the stimulation. The co-processor seeks to effectively bridge across the lesion, forward propagating the object shape and task structure information, indirectly, through the use of stimulation.

In our experiments below, we demonstrate our co-processor design on three types of simulated lesions:

- **Output-based AIP:** we force the output of some proportion of "AIP" neurons to zero, effectively removing them from the network. This results in a loss of object shape information.
- **Connection-based:** we prevent the propagation of information between the "F5" and "M1" modules, effectively representing a severing of the connections between the two. Note that the sparse connections between them run both directions, and we are lesioning both.
- **Output-based M1:** we force the output of some proportion of "M1" neurons to zero, causing a more holisitic loss of movement. Here, the lesion may make

it impossible for the co-processor to find a solution, but some recovery may be possible.

3.2.2. Simulated network exhibits long running dynamics Just as the co-processor must adapt to the lesion, it must also adapt to the dynamics of the network it is stimulating. Natural neural networks as well as our simulated network exhibit long running dynamics, which our CPN and EN must account for in their learning. A perturbation of a network (i.e. due to stimulation) will cause changes in neuron activations long after the stimulation is applied, sometimes far from the site of stimulation. Our simulated grasping circuit exhibits the same behavior.

To illustrate this, suppose we applied a small, one-time, instantaneous perturbation of the hidden state of 10 randomly chosen neurons in the output (M1) module at some point in time during a trial. If we repeat that experiment many times, we can see what the distribution of long-running effects tends to look like on the output muscle velocities.

In Fig. 4 we can see that even a single, one-time perturbation in the network has effects dozens of time steps later. Our co-processor will need to account for these dynamics, since stimulation is intended to cause perturbations in a network. As we will show in the next subsection, the problem the co-processor faces is in-fact even harder than this, due to a stimulation model that includes both spatial and temporal smoothing.

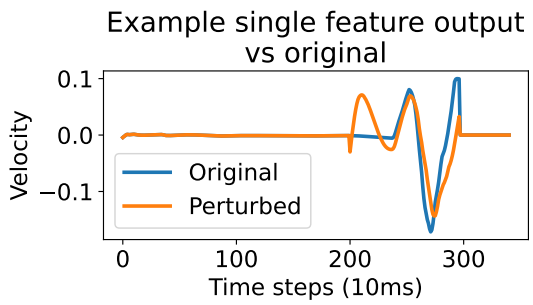

(a) Example trial

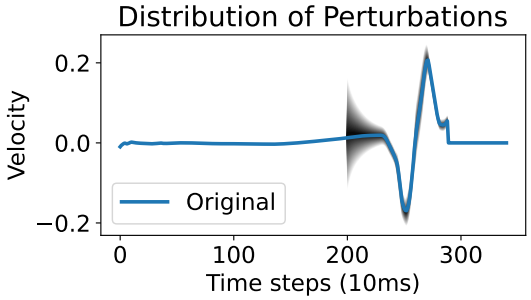

(b) Distribution of effects across n=1000 samples. Greyscale field represents variance across samples.

Figure 4: Instantaneous perturbations of a random sample (n=10) of M1 neurons at time t=200 results in long-running effects on output.

3.2.3. Stimulation model In order to include another aspect of realism in our simulation, we subject the co-processor to a stimulation model, rather than allowing it to directly influence the hidden state of the simulated network's neurons. Our stimulation model includes aspects of both spatial and temporal smoothing.

The intent with this approach is not to create a realistic biophysical model. The mRNN model does not contain sufficient information to arrange the neurons in a

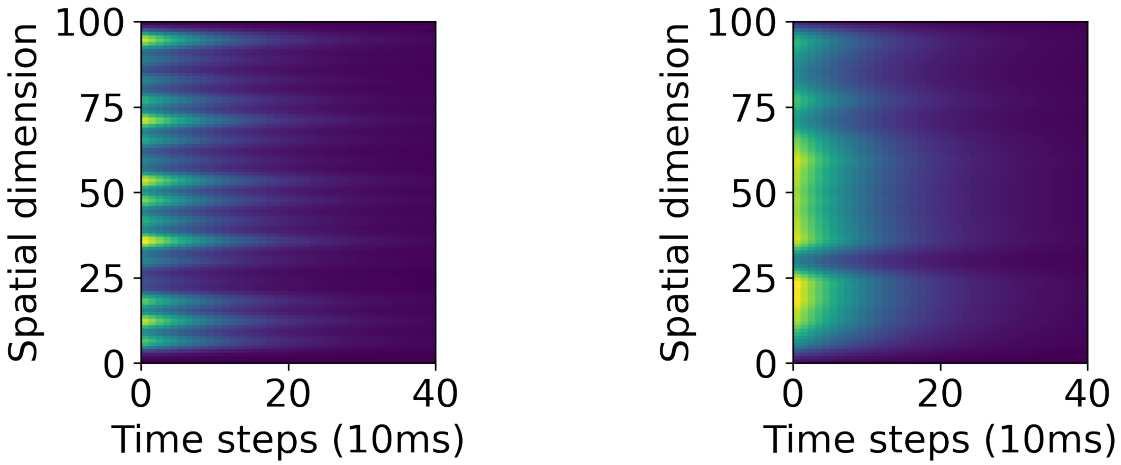

(a) $\sigma = 1.875$ (b) $\sigma = 2.875$

Figure 5: Spatial and temporal smoothing of a single 16 dimensional, randomized θ, onto 100 simulated neurons. Color values indicate the magnitude of the value summed into each neuron's hidden state in that time step. After $t = 0$, θ is the zero vector.

simulated space, and to simulate how that may change the effects of stimulation. Instead, our stimulation model is merely attempting to make the co-processor's task more realistically difficult, in the sense that it cannot precisely set the hidden state of every neuron, instantaneously and in each time step. Any stimulation it applies will diffuse across "space" and time.

In our experiments, we stimulate only the output module, since this co-processor's purpose is to improve external task performance, which it is able to do with only stimulation of the output module of the network. It is conceivable that a co-processor could stimulate other areas of the brain to improve task performance downstream, or to probe the brain to better reveal the user's intent (i.e. object shape), but we did not explore those possibilities in this paper.

The stimulation function S receives as inputs the stimulation parameters θ provided by the CPN, which it accumulates in an internal memory. Each time step, it outputs a modifier to the internal states of all neurons in the output module, based on the current state of memory. That memory allows the stimulation function to perform temporal smoothing. Specifically, we used a simple exponential decay model where the function reads its current state of memory, sums in the new parameters, and then decays each memory element towards 0.0 at some rate. Roughly speaking, this design intends to approximate the notion of dissipation: the effect of stimulation is not instantaneous, but rather decays with time, as charge dissipates into the surrounding area.

Likewise, the stimulation function maps the relatively low dimensional stimulation parameter vector θ onto the M1 cells which it stimulates. In our experiments, our stimulation parameters θ had 16 dimensions, which we found was sufficient to allow

significant improvement in task performance. The stimulation function uses a simple Gaussian smoothing to map those parameters onto the simulated M1 neurons. Each parameter represents, in a sense, an electrode located along a single spatial dimension, whose stimulation affects the neurons in its vicinity more than it affects others, according to each neuron's Mahalanobis distance from it. The neurons are aligned along that dimension arbitrarily. We fix the width of the Gaussian distributions arbitrarily to $\sigma = 1.75$. We are not aware of a principled way of picking this value, and clearly if we set it to extreme values, it makes our simulation less useful. For example, if it is set to an extreme high value, the stimulation is effectively lower dimensional, resulting in a model corresponding to a stimulation technology that is inappropriately low resolution for our task, for example epidural stimulation. We could not conclude much from such an experiment, because this simulation does not constitute a biophysical model, where we can identify some realistic value. The purpose of this smoothing technique is only to make the co-processor's job harder in the simple sense that it cannot target neurons individually. As a result, we set it to a moderate, balanced value, and don't vary it.

Thus, the governing equations of the stimulation become:

$$\alpha_t = \tau\alpha_{t-1} + \theta_{t-1} \tag{1}$$

$$s_t = C(\alpha_t) \tag{2}$$

- α: the 16 dimensional internal activation, or memory of our stimulation
- τ: our decay rate, which we set arbitrarily to 0.7
- C: a precalculated $100x16$ matrix which provides our Gaussian smoothing
- s_t: the stimulation we apply to each neuron at the given time step.

The governing equations of the simulated network then become:

$$x_{t+1} = Jx_t + Iv_t + s_t + b \tag{3}$$

$$a_t = tanh(x_t) \tag{4}$$

$$y_t = La_t + l \tag{5}$$

- x: the hidden state of each neuron
- J: the recurrence weight matrix
- I: the input response matrix
- v_t: the visual input vector
- b: the neuron activation bias
- L, l: the parameters of the linear readout
- y: the output of the network

See Fig. 5 for a visual depiction of an example where θ is non-zero at $t = 0$, and zero for all other times, in order to see how stimulation is applied across space and time. In Fig. 6, we see stimulation applied during the simulation, in a real trial. In this case, the trial is one where 50% of M1 neurons are lesioned to have zero output. Observations of the network's hidden state (explained in the next section) are taken from the first two modules, and stimulation is applied to the last module. This fact is intended to capture the difficulties with observing the same region that you are stimulating, due to stimulation artifacts. The trial we show depicts stimulation supplied by a highly trained co-processor, where task performance has been significantly restored. We explain this experiment in more detail below.

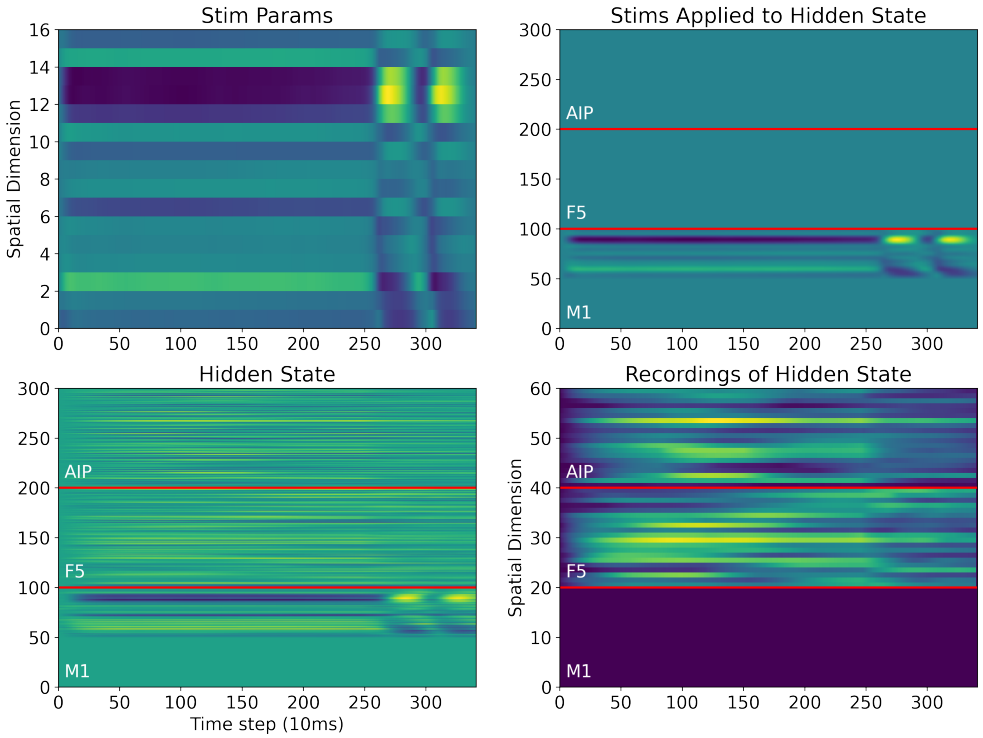

Figure 6: Example of stimulation and observation for a single trial. Here, M1 has been lesioned 50%, as seen in the zero (light blue) hidden states. We gather observations only from the AIP and F5 modules, as we explain in Section 3.4. Stimulation is applied to M1, to drive the network output.

3.2.4. Observation model Our observation model likewise relies on a notion of electrodes spread along a single spatial dimension. As with stimulation, this is not intended to capture true physical relationships between neurons and electrodes, but rather to act as a dimensionality reduction that isn't designed to specifically favor task

success, such as PCA. We treat the neurons of each module as occupying their own space, with 20 electrodes arrayed along each.

We use a similar Gaussian-based approach as with stimulation, but in this case our approach looks much like a Gaussian convolution, where the Gaussian kernel is centered at each electrode position. Each 'electrode' is read out as a weighted average of all neurons in the given module, with weights being provided by the Gaussian kernel. As above, refer to Fig. 6 for a visual example.

3.2.5. Brain co-adaptation To demonstrate the co-processor's ability to adapt to the non-stationarity of the brain, we also change the brain throughout the co-processor's training. Specifically, we simulate the brain's co-adaptation with the stimulation to cooperatively solve the problem, as the stimulation is also changing through the CPN's training.

We achieve this through a simple error backpropagation, using PyTorch's implementation of the *Adam* optimizer. With each trial, task loss is calculated and backpropagated into the mRNN, allowing it to adapt to the fact it receives stimulation. The learning rate for the optimizer is set arbitrarily to a relatively low rate of $1e^{-7}$. The learning rate was not chosen in a principled way, since we are not aware of a principled way of choosing it. However, we reason that it should be lower than the co-processor by orders of magnitude due to the rapidity with which an ANN can be retrained in practice.

3.2.6. Simulating recovery prior to co-processor use We sought to additionally re-train the mRNN after applying the lesion in order to simulate stroke recovery. For our simulated lesions which zero the outputs of neurons, the mRNN cannot supply an appropriate pre-recovery model. We know that strokes can cause damage from which the subject, in many cases, cannot recover. The mRNN model has sufficient redundancy built into it that lesioning the outputs of large numbers of neurons often leaves enough remaining degrees of freedom that a nearly full recovery can occur, unless so many neurons are lesioned that no stimulation could be effective.

We can, however, simulate pre-recovery in the case of a lesion that prevents communication between the F5 and M1 modules. In that case, object shape information cannot propagate forward in the network, in order to condition the hand for grasping. The mRNN can, in pre-recovery, learn a stereotyped grasp. After that point, the co-processor's job will be to forward-propagate object shape information to specialize that grasp for the individual objects. We explore this in one of our experiments, explained below.

3.2.7. Simulating a non-stationary observation function, e.g. sensor drift We also demonstrate the co-processor's ability to adapt to non-stationarity in the observation function. Over time, implanted sensors may drift from true readings. To test the co-processor's ability to adapt to that drift, we perform an experiment where the

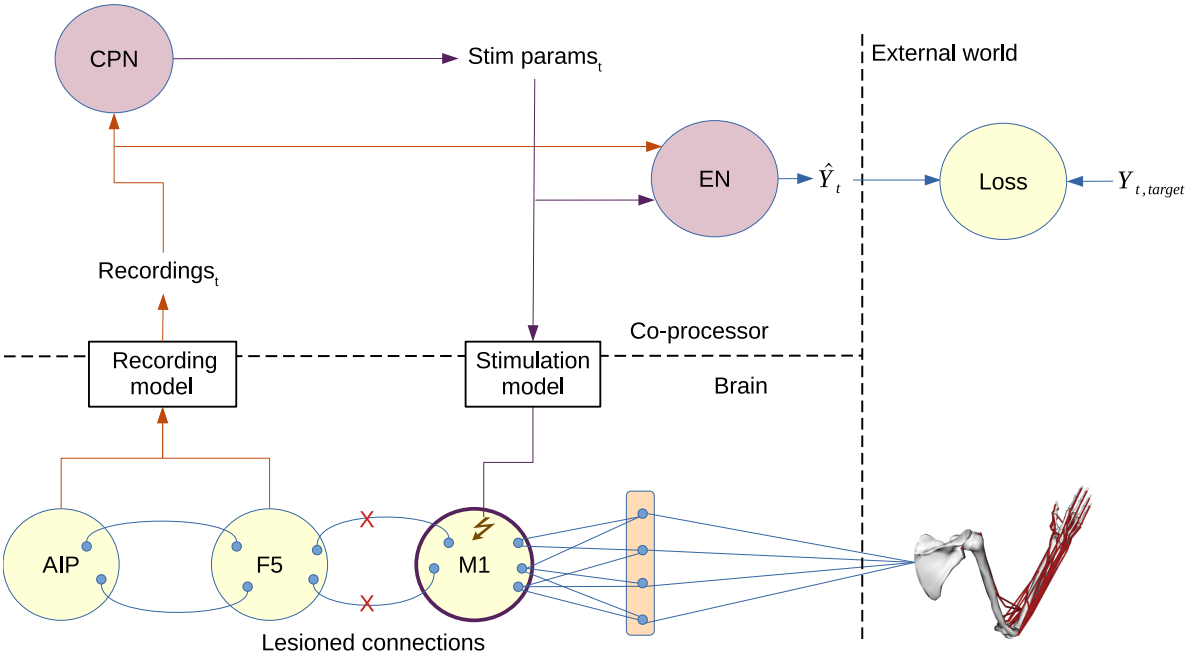

Figure 7: Experiment architecture overview

observation function has a bias term which changes over time, according to a random process. Each epoch, we add a random value to each element of the bias, drawn from a mean-0 Gaussian distribution. That causes the "sensors" to have a drifting zero point over time. See Supplement 9.2 for further details.

3.3. Training Algorithm

In all experiments, training the co-processor requires a careful interleaving of EN and CPN training epochs. EN training epochs concentrate on updating the EN, based on observations of the effect of stimulation on the simulated network's output, and comparing it to the EN's predictied output. The loss function when training the EN is the mean squared error (MSE) loss between the actual and predicted output of the mRNN (i.e. muscle velocities). We then use the EN to train the CPN during the CPN training epochs. During that time, we backpropagate the MSE loss between the EN's predicted output, and target output, to the CPN. In other words: we treat the EN's output as a proxy to the true brain, allowing us to train the CPN, since we have no way to "backpropagate through the brain" itself. See Fig. 8.

3.3.1. EN training For the EN to be useful, it must accurately predict the effect of stimulation produced by the CPN. In addition to that, backpropagating through it must yield gradients which train the CPN to output more useful stimulation. We discovered that this latter property does not occur simply by virtue of the former. An EN of this design can be trained to high levels of predictive power, even on random stimulation, and to orders of magnitude lower loss than the task loss, while at the same

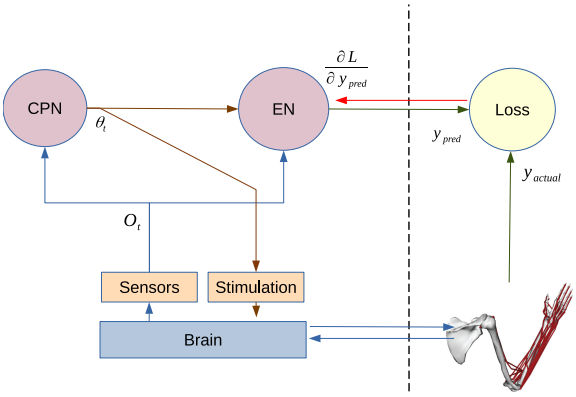

(a) EN training phase: backpropagate actual vs predicted

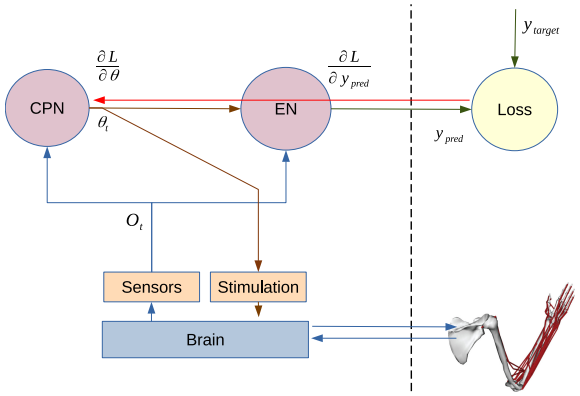

(b) CPN training phase: backpropagate actual vs target MSE loss, via EN, to CPN. This effectively treats the EN output as the actual, and thus the EN must be trained first.

Figure 8: Two Phase Training Regime

time backpropagation through it yields gradients which are not useful for training the CPN. As a result, if the EN is not trained in specific ways, the CPN exhibits unstable training. We have thus far been unable to discover a way to measure and optimize for this second property directly, though pursuing it may be a fruitful subject of future applied ML research. Instead of attempting to train an EN directly to exhibit this property, we discovered a training regime that indirectly, but reliably, makes it occur.

The central concept of our training regime is to provide a carefully chosen variety of training examples, and to use heavy weight regularization, in order to force the EN to generalize well to stimulation which it hasn't yet seen. We hypothesize that the crux of our EN training problem is one of over-fitting: that the EN may be trained to high predictive power on a set of stimulation examples, but that the effective dimensionality of the problem it is learning is comparatively quite high, due to both the dimensionality of our stimulation parameters θ, and the dynamics of the network being stimulated. As a result, the hypersurface which it fits to the training examples may exhibit gradients not reflective of reality.

First, and most significantly, we structure the training dataset for each EN training epoch in a very specific way. Each epoch, we include:

- examples using stimulation from the current CPN
- examples from a small (100s) collection of CPNs which are copies of the current CPN, with Gaussian-distributed mean-0 noise added to their parameters
- examples of white noise stimulation

We developed this structure under the belief that we needed to cover a sufficient variety of examples to prevent overfit, and to do so in a way that emphasizes the neighborhood in CPN parameter space of the current CPN. We initially attempted to pad our dataset with white noise examples alone, but that was not sufficient to stabilize CPN training,

despite the EN's ability to reach a high predictive power. Adding in the addition of samples from the parameter space near the current CPN appears to help ensure that the EN is localized enough to give useful gradients for that area. As we will explain below, this produces an additional problem that the EN is too specialized to the local area of CPN parameter space, but we then solve that problem using EN retraining, interleaved with the CPN training.

After some experimentation, we composed each batch of EN training data in the following way:

Source	**Proportion of dataset**
Current CPN	10%
Current CPN with parameter noise	60%
White noise stimulation	30%

Additionally, we use PyTorch's *AdamW* optimizer, which includes an option for weight regularization. With that, we use a carefully chosen learning rate schedule. Our intuition is to leverage regularization as one of the standard mitigations for overfit. To converge, the learning rate schedule needs to be chosen carefully: a relatively high learning rate at first, dropping to a very low rate soon thereafter. Using too-low or too-high of a learning rate in any phase causes the EN learning to not converge. EN training proceeds until it reaches a threshold of prediction error, defined as a fraction of the current CPN's task loss.

3.3.2. CPN training Once an EN is properly trained, CPN training is straightforward. For this phase, we generate training examples using the current CPN alone. The EN generates predictions of the effect of those stimulations, and we backpropagate through the EN to generate training gradients for the CPN. As with the EN, we constitute the dataset with a large random sample of trials from the original Michaels task. See Fig. 8.

The choice of learning rate schedule for training the CPN is somewhat important. The CPN appears to train in two phases. In the first phase, it is largely learning the structure of the reach-to-grasp task, e.g. that the muscles need to stay still until the reach begins. During that phase, the learning rate can be quite high. Later, the CPN begins to learn the mapping between the object shape information observed from the simulated brain, and how that should map onto stimulation. That phase of the training requires a learning rate 2-3 orders of magnitude lower than in the first phase. We will cover this in some more detail in the Results section (Section 4).

3.3.3. Interleaved CPN/EN training, and adapting to non-stationarity Having defined the training procedures for the EN and CPN, we can define a training algorithm combining those two. We train the two in alternation, creating a new EN each time we enter an EN training phase. We explored the possibility of reusing an existing EN by retraining it, for the purpose of training efficiency. However, we found that retraining an

EN was no more fast than training a new one, and in-fact usually took longer, despite significant experimentation with learning rates. It is unclear if that fact is an artifact of our simulation, or of the problem more generally, and so it needs more examination in the future, for the purpose of training efficiency.

The key remaining challenge at that point is determining when an EN is no longer suitable for training the current CPN. Expiring an EN at the right time accomplishes two things. First, it ensures that our current EN is trained properly for the current CPN; without that, the CPN training will become unstable. Second, expiring the EN is how we adapt our learning to the brain's non-stationarity. At some point, the brain will have changed sufficiently for our EN to be out-of-date, and therefore requiring replacement.

We solve this challenge through a simple set of metrics, which, when satisfied, indicate we need to transition to an EN training period. Our first metric simply captures the EN's declining predictive power. When the EN's prediction error reaches a point which is sufficiently above some ratio to the CPN's task loss, we expire the EN immediately. Second, we expire the EN if CPN loss does not improve (or gets worse) across a sufficient number of recent training steps. This resembles common stopping conditions in iterative learning: one stops when learning is no longer improving the model. Together, these two metrics appear effective in ensuring we expire the EN at the right time. See Supplement 9.1 for additional details.

3.4. Experiments

Using the simulation described above, we perform several experiments to demonstrate the co-processor's ability to learn. In each experiment, we apply one of the three lesion types described above. We additionally vary whether we simulate brain co-adaptation, in order to understand its impact on the co-processor training. Additionally, we perform one experiment where we attempt to simulate natural recovery from the lesion, prior to training the co-processor. Our final experiment includes sensor drift, as well as co-adaptation. In sum, our experiments are:

	Lesion	**Simulate co-adaptation?**	**Simulate pre-recovery?**	**Simulate sensor drift?**
1	50% AIP loss			
2	50% AIP loss	X		
3	50% M1 loss			
4	50% M1 loss	X		
5	100% connection loss F5<->M1			
6	100% connection loss F5<->M1	X		
7	100% connection loss F5<->M1	X	X	
8	100% connection loss F5<->M1	X		X

In each experiment, we use a single mRNN model, sourced directly from the results cited in Michaels [2]. We drive the experiment using the same set of input and output data that the mRNN was trained on. The dataset contains a total of 502 trials, spread uniformally among 42 object classes. In each experiment, we separate a random sample of 20% of the dataset for validation.

3.5. Stopping condition

For the purpose of these experiments, we train the co-processor until one of two conditions is satisfied:

- The percent change in task loss between two consecutive 500 epochs is below a certain threshold: 0.01%. This stopping criteria ensures we stop training when the economy of additional training is low.
- The epoch count is greater than 250k. This criteria provides a backstop against very slow training running without end.

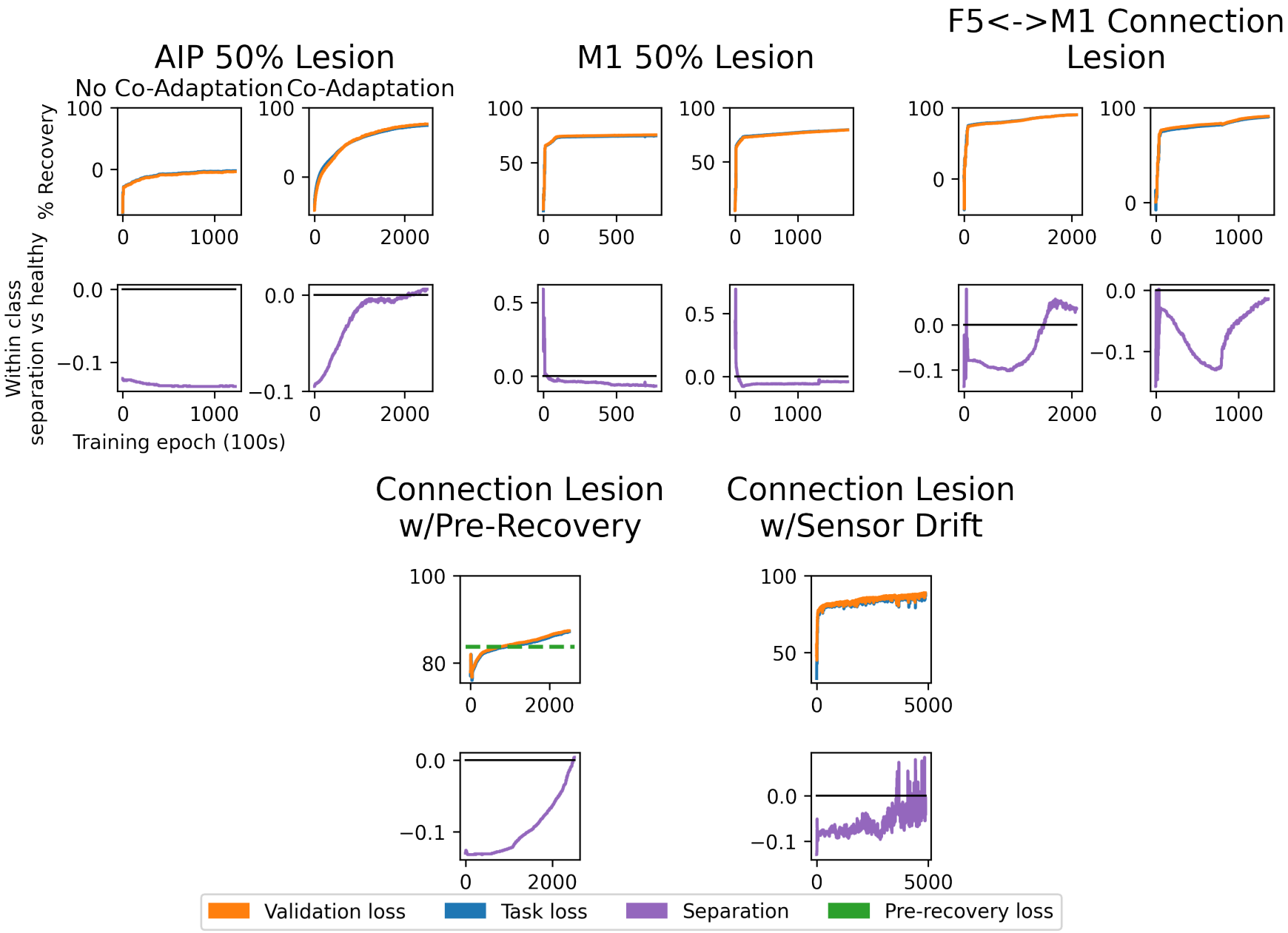

Figure 9: Loss and class separation vs training epoch

4. Results

With each experiment, we track two metrics to characterize the learning progress. First, we track the task loss, which is an MSE loss that measures the co-processor's ability to restore movement towards the target trajectory. We define it over the muscle length trajectory vector output from the simulated network, compared to the ground truth muscle length data captured during the Michaels experiment. In graphs, we characterize this loss measure in terms of its percent recovery - i.e. difference from lesioned and healthy performances. See Fig. 9, and Table 1 for detailed results.

Second, we measure the degree to which the co-processor's solution successfully differentiates object classes. We measure the ratio of within-class and total variation, and compare that to the healthy network. Our separation metric S is defined as:

$$S = \frac{\sigma_a}{\sigma_w} - \frac{\sigma_{a,h}}{\sigma_{w,h}} \tag{6}$$

where σ measures the mean variation, across time, and across all data points in a given sample. σ_a is the total variation of a dataset, and σ_w is the average of the within-class variations. The h indicates the healthy metric. An S value of 0.0 indicates that the grasps for the various object classes vary to the same degree as the healthy network.

This metric S allows us to differentiate overall task performance improvement and the ability of the co-processor to condition the grasp based on visual information. To successfully grasp in the real world, the hand must be preformed appropriately for the shape of the object being grasped, and must close around it appropriately. The structure of the delayed reach-to-grasp task can be learned by the co-processor, e.g. to hold muscle velocities to 0.0 for the initial part of each trial, without it also learning to differentiate the various object shapes from the brain observations. Roughly speaking, S is our metric for differentiating overall decrease of task loss, and improvement in object differentiation.

4.1. Experiment 1: AIP 75% lesion

This experiment demonstrates the ability for the co-processor to succeed after the patient has lost some of the neural machinery responsible for representing the objects' shapes. In the non-coadaptive version of this experiment, the loss of AIP neurons involved in encoding the visual inputs results in the simulated brain being unable to condition its grasp for the object shape, though reaching largely still succeeds. Note in Supplement 9.3 that lesioned loss is lower in this experiment than in others: the user continues to reach successfully, but not to form the hand properly, as explore above. Likewise, the co-processor doesn't have sufficient information to improve performance, for lack of that information.

In the co-adaptive case, the brain and co-processor find a solution that largely recovers performance. This demonstrates that the co-processor can adapt to the

non-stationarity of the mapping between the observed brain activity and the optimal stimulation. Note, though, that the simulation is not designed to indicate if the co-processor speeds up recovery, or provides better results than natural recovery.

Additionally, in Fig. 9 we see that initially the co-processor and brain did not strongly separate the object classes, but that they learned to as the training proceeded. This is again due to the co-processor and brain learning how to map the input visual information on to the task.

4.2. Experiment 2: M1 50% lesion

In this experiment, 50% of the output module of the simulated network has been lesioned. In the co-adaptive case, the co-processor needs to adapt to non-stationarity in the mapping between stimulation and task performance. In the non-coadaptive case, training quickly plateaus, and does not improve thereafter. That suggests we have lost some of our degrees of freedom to control the activations in the output layer, resulting in a reduced ability to recreate the target grasps.

In the co-adapative case, performance likewise hits an inflexion point, but continues to improve slowly. The ability to improve further is tied to the simulated recovery restoring the degrees of freedom needed for success. The co-processor in this later phase of training must adapt to the non-stationarity that results from that recovery process, which it does successfully.

4.3. Experiment 3: F5 and M1 connection lesion

As in the other cases, the co-processor's loss in this experiment improves quickly, initially, but takes much longer to refine. During that refinement, object differentiation occurs. Note that in this experiment, no information can propagate forward to the M1 module, or backwards from it, since we have completely severed the inter-module connections involving that module. It is the sole responsibility of the co-processor to perform that forward-propagation.

In this case, co-adaptation only affects the M1 module, since we have nothing to use as a learning signal: there is no "backpropagation" to the AIP and F5 modules. As a result, this experiment demonstrates that the co-processor's learning algorithm is capable of adapting to non-stationarity in the mapping between stimulation parameters and task performance. Contrast that with the results of Experiment 1, where the non-stationarity affected the mapping between the visual inputs and the brain observations.

Object separation is initially low and unstable, as the co-processor begins to learn the task. Afterwards, it stabilizes as the co-processor begins to leverage observed brain activity to differentiate object shapes. In that phase of training, the object separation eventually begins convergence towards healthy activity.

4.4. Experiment 4: Connection lesion with pre-recovery

In this case, we simulate some amount of recovery prior to the co-processor learning. Complete recovery is impossible, because the output module's connections to F5 (both forward and backward) are masked. As a result, the pre-recovery causes the simulated brain to learn an object-agnostic stereotyped grasp. The co-processor's job is to forward-propagate the information necessary to condition the grasp on the object shape.

The co-processor in this scenario successfully improved task performance beyond the recovery point. Note that the object class separation metric S returned to a healthy value towards the end of the training, indicating that the learned solution did not simply refine the stereotyped grasp.

4.5. Experiment 5: Connection lesion with sensor drift

Here we simulate sensor drift, using the same connection lesion above, and co-adaptation. As in the other connection lesion experiments, the co-processor learns the reach-to-grasp task, and forward-propagates visual information to condition the grasp. Notably, because the observation function is non-stationary in this experiment, the class separation exhibits far higher epoch-to-epoch variance in the later epochs. The co-processor presumably becomes more reliant on upstream visual information over time, as it learns how to map it on to the task. As a result: it becomes more sensitive to upstream non-stationarity as it learns. That is - earlier training epochs involve learning the task structure - i.e. delayed reach-to-grasp - but in a largely object-agnostic sense. Later, it further leverages the observations in order to differentiate object shapes. Note however that it continues to perform well in later epochs in terms of task loss.

We present the results of this experiment without our stopping condition applied, due to the noise in the training causing stoppage while results are still improving. For this experiment, we opted instead to stop training after running the experiment long enough to get results near to the version of this experiment without sensor drift.

Note also that training efficiency was, unsurprisingly, decreased relative to the experiment without sensor drift. For example, the sensor drift version required $282k$ training epochs to reach 85% recovery, whereas the version without sensor drift required only $93k$.

5. Discussion and Future Work

We present here a first-of-its-kind demonstration of a novel design for neural co-processors, allowing for an AI agent to learn neural stimulation policies that improve a user's performance of an external task. The design revolves around the use of a stimulation model for training the agent, providing a proxy to the true function mapping stimulation and neural activity to task performance. We base our demonstration on a simulation of a neural circuit engaged in an external grasping task.

Our co-processor design adapts well to a variety of simulated lesion types, reducing task loss 75-90% across our various experiments. To work this well, the co-processor needed to adapt to the long-running dynamics of the simulated network, as well as the long-running effects of stimulation. In some experiments we required it to additionally adapt to non-stationarity in the neural circuit, which was actively changing at the same time the co-processor was learning. It achieved that as well, co-adapting with the simulated brain to improve external task performance. It also adapted to a simulated brain which had already undergone some amount of lesion recovery. In that case, the co-processor successfully identified the information upstream from the lesion which was necessary to stimulate the motor cortex downstream. Finally, it was able to adapt to simulated sensor drift, though with a penalty to training efficiency.

Clearly, we need to discuss carefully what can and cannot be inferred from simulation studies such as these. An example of such a simulation approach is Dura-Bernal et al. [35]. In this work, the authors use a simulated spiking neural network to train a stimulation agent. Their stimulation agent sought to restore the network's control of a simulated arm, to reach a target, after a simulated lesion was applied, much like the work here. As the authors point out, we have a limited ability to probe a neural circuit *in vivo* in order to perform learning. As a result, we first need to design our approach through the use of an admissible simulation. The authors in this case simulated lesions by effectively removing parts of their simulated network, or by cutting connections between parts of the network. Here, we use an established design for an artificial neural circuit which performs a grasping task. Its architecture and training methods were designed specifically to result in naturalistic dynamics.

As in Dura-Bernal [35], we note that our simulation differs drastically from an organic brain, both in scale and structure. Today, predicting long-running neural responses to stimulation remains a difficult problem, implying targeted neural control is also difficult. Even moreso, identifying the neural correlates of complex task success remains largely out of reach [23]. What, then, does our simulation provide us?

Abstractly, the co-processor lends itself to any closed-loop neural stimulation problem where a relevant stimulation model can be identified. There are many lower dimensional problems today which we address with far simpler stimulation regimes than would be necessary for e.g. fine-grained finger control. In some applications, such as PD symptom relief, stimulation is often parameterized by a single off-vs-on parameter, or a small handful of parameters, where the key challenge is learning when to apply the stimulation, and its shape and power. Our simulation demonstrates the ability of our training method to adapt to higher dimensional problems than these, where additionally the long-running effects of stimulation on the intended figure-of-merit must be modeled. These properties together suggest it may be useful in lower dimensional problems where a stimulation model can be estimated, and stimulation parameters can be tied to the target objective.

Our future work will include a reinforcement learning (RL) approach, where the co-processor explicitly learns when to apply stimulation, in addition to parameterizing it.

Its target objective involves not only symptom relief, but also minimizing energy use. In this approach, our CPN and EN may correspond to the Actor and Critic portions of an Actor-Critic model for example. Here, the Critic would learn to value symptom relief, while attaching a cost to stimulation, thus incentivizing an energy efficient approach.

One challenge remaining with our current co-processor design is training effiency. On the whole, the co-processor quickly improved task performance, but required orders of magnitude more training examples to achieve its highest levels of performance. Even moderate amounts of recovery may be valuable to a user, but nevertheless we consider training efficiency to remain a problem. Due to limits on patient fatigue, time, implant battery life, and other concerns, it is not plausible to expect a learning algorithm to have access to unlimited amounts of training data. As a result, it is necessary to make efficient use of the data we can acquire. We believe there exist at least three mitigations for that:

- Retraining an existing EN, rather than regularly creating a new one. As mentioned above, we encountered difficulty with this approach, but it remains to be seen if this is a fundamental problem with our training method, rather than a peculiarity of our simulation. Also, it remains unclear if a solution for our simulation exists as well, which we've simply yet to identify. This remains a future area of inquiry.
- Making better use of what data we acquire. In this initial simulation we do not retain data beyond the present training epoch. In practice, we can likely retain training data for some time window. Non-stationarity requires us to regularly discard or discount data as it ages. However, in practice, training epochs operate on the order of seconds, suggesting that data can be retained and reused for multiple epochs. The 'speed' of non-stationarity compared to the co-processor's learning therefore must be an area of future research.
- Matching the dimensionality of the stimulation and observations to the amount of available data. If one chooses a stimulation regime with a small number of controllable parameters, where nevertheless task improvement from the stimulation is possible, that allows for a simpler co-processor which will likely require less training data.

Having now demonstrated our method on a higher dimensional problem, we will next demonstrate it on a lower dimensional problem, one which is likely to transfer more readily to an *in vivo* trial. We hypothesize that this co-processor model will transition well to applications in PD, or essential tremor (ET). In Castaño-Candamil et al. [25], we see an ML-based approach to closed-loop stimulation for ET relief. Here, a simple learning model extracts neural markers (NMs) from a human patient's M1 cortex. It uses those to condition DBS stimulation parameters. The stimulation controller adapts to non-stationarity of the mapping between NMs and optimal control, which is necessary due to the sensitivity of NMs to context (e.g. sitting or standing). The co-processor model is likely to transition well to such an application, where it may provide additional energy savings or reduction of stimulation side-effects. In that case, it will attempt to

extract neural markers appropriate for each context, to detect transitions in context, and to apply optimal stimulation.

6. Conclusion

We have demonstrated a general framework for training a closed-loop neural stimulator, called a "neural co-processor". We outlined one specific co-processor design, and outlined an approach to training it using supervised learning. In simulation it successfully learned to alleviate some of the effects of a brain lesion. To do so, it needed to co-adapt with the simulated brain, which exhibited non-stationarity. Additionally, it needed to learn long-running effects of the stimulation it learned to apply. Because of these properites, the co-processor approach likely generalizes well to a wide range of clinical applications where closed-loop neural stimulation is appropriate.

7. Acknowledgements

This work was supported by a Weill Neurohub Investigator grant, a CJ and Elizabeth Hwang endowed professorship (RPNR), and National Science Foundation grant no. EEC-1028725.

The authors would like to thank the following for discussions and insights related to the present topic:

- Karunesh Ganguly, UC San Francisco
- Priya Khanna, UC Berkeley
- Anca Dragan, UC Berkeley
- Justin Ong, University of Washington
- Luciano De La Iglesia, University of Washington

8. References

[1] RPN R 2019 *Current Opinion in Neurobiology* **55** 142–151

[2] Michaels J, Schaffelhofer S, Agudelo-Toro A and Scherberger H 2020 *Proceedings of the National Academy of Sciences* **117** 32124–32135 ISSN 0027-8424 (*Preprint* https://www.pnas.org/content/117/50/32124.full.pdf) URL https://www.pnas.org/content/117/50/32124

[3] Rao R 2013 *Brain-Computer Interfacing: An Introduction* (Cambridge University Press) ISBN 9780521769419

[4] Wolpaw J and EW W 2012 *Brain-Computer Interfaces: Principles and Practice* (Oxford University Press)

[5] Moritz C, Ruther P, Goering S, Stett A, Ball T, Burgard W, Chudler E and Rao R 2016 *IEEE transactions on bio-medical engineering.* **63**(7) 1354–1367

[6] Lebedev M and Nicolelis M 2017 *Physiological reviews* **97**(2) 767–837

[7] Walker E e a 2019 *Nature Neuroscience* **22**(12) 2060–2065 URL https://doi.org/10.1038/s41593-019-0517-x

[8] Niparko J 2009 *Lippincott Williams and Wilkins* (Oxford University Press)

[9] Weiland J and Humayun M 2014 *IEEE transactions on bio-medical engineering* **61**(5) 1412–1424

[10] Tomlinson T and Miller L 2016 *Advances in experimental medicine and biology* **957** 367–388

[11] Tabot G A, Dammann J F, Berg J A, Tenore F V, Boback J L, Vogelstein R J and Bensmaia S J 2013 *Proceedings of the National Academy of Sciences* **110** 18279–18284 ISSN 0027-8424 (*Preprint* https://www.pnas.org/content/110/45/18279.full.pdf) URL https://www.pnas.org/content/110/45/18279

[12] Tyler D 2015 *Current opinion in neurology* **28**(6) 574–581

[13] Dadarlat M, O'Doherty J and Sabes P 2015 *Nature neuroscience* **18**(1) 138–144

[14] Flesher S N, Collinger J L, Foldes S T, Weiss J M, Downey J E, Tyler-Kabara E C, Bensmaia S J, Schwartz A B, Boninger M L and Gaunt R A 2016 *Science Translational Medicine* **8** 361ra141–361ra141 (*Preprint* https://www.science.org/doi/pdf/10.1126/scitranslmed.aaf8083) URL https://www.science.org/doi/abs/10.1126/scitranslmed.aaf8083

[15] Cronin J, Wu J, Collins K, Sarma D, Rao R, Ojemann J and Olson J 2016 *IEEE transactions on haptics* **9**(4) 515–522

[16] O'Doherty J, Lebedev M, Ifft P, Zhuang K, Shokur S, Bleuler H and Nicolelis M 2011 *Nature* **479**(7372) 228–231 URL https://doi.org/10.1038/nature10489

[17] Yang Y, Qiao S, Sani O, Sedillo J, Ferrentino B, Pesaran B and Shanechi M 2021 *Nature Biomedical Engineering* **5**(4) 324–345 URL https://doi.org/10.1038/s41551-020-00666-w

[18] Tafazoli S, MacDowell C, Che Z, Letai K, Steinhardt C and Buschman T 2020 *Journal of Neural Engineering* **17** 056007 URL https://doi.org/10.1088/1741-2552/abb860

[19] Benabid A 2003 *Current opinion in neurobiology* **13**(6) 696–706

[20] Holtzheimer P and Mayberg H 2011 *Annual review of neuroscience* **34** 289–307

[21] Kisely S, Hall K, Siskind D, Frater J, Olson S and Crompton D 2014 *Psychological medicine* **44**(16) 3533–3542

[22] Fraint A and Pal G 2015 *Frontiers in Neurology* **6** 170 ISSN 1664-2295 URL https://www.frontiersin.org/article/10.3389/fneur.2015.00170

[23] Khanna P, Totten D, Novik L, Roberts J, Morecraft R and Ganguly K 2021 *Cell* **184**(4) 912–930 URL https://pubmed.ncbi.nlm.nih.gov/33571430/

[24] Bosking W, Beauchamp M and Yoshor D 2017 *Annual review of vision science* **3** 141–166

[25] Castaño-Candamil S, Ferleger B I, Haddock A, Cooper S S, Herron J, Ko A, Chizeck H J and Tangermann M 2020 *Frontiers in Human Neuroscience* **14** 421 URL https://www.frontiersin.org/article/10.3389/fnhum.2020.541625

[26] Little S e a 2016 *Journal of neurology, neurosurgery, and psychiatry* **87**(7) 717–21

[27] Berger T, Song D, Chan R, Marmarelis V, LaCoss J, Wills J, Hampson R, Deadwyler S and

Granacki J 2012 *IEEE transactions on neural systems and rehabilitation engineering : a publication of the IEEE Engineering in Medicine and Biology Society* **20**(2) 198–211

[28] Kahana M J e a 2021 *medRxiv* (*Preprint* https://www.medrxiv.org/content/early/2021/05/22/2021.05.18.212569 URL https://www.medrxiv.org/content/early/2021/05/22/2021.05.18.21256980

[29] Bolus M, Willats A, Rozell C and Stanley G 2021 *Journal of neural engineering* **18**(3)

[30] Kim L Y, Harer J A, Rangamani A, Moran J, Parks P D, Widge A S, Eskandar E N, Dougherty D D and Chin S P 2016 *2016 38th Annual International Conference of the IEEE Engineering in Medicine and Biology Society (EMBC)* 808–811

[31] Güçlü U and van Gerven M 2017 *Frontiers in computational neuroscience* **11**

[32] Sussillo D, Churchland M, Kaufman M and Shenoy K 2015 *Nature Neuroscience* **18**(7) 1025–1033

[33] Simonyan K and Zisserman A 2015 Very deep convolutional networks for large-scale image recognition *International Conference on Learning Representations*

[34] Puthenveettil S, Fluet G, Qiu Q and Adamovich S 2012 *Annual International Conference of the IEEE Engineering in Medicine and Biology Society. IEEE Engineering in Medicine and Biology Society. Annual International Conference* **2012** 4563–4566

[35] Dura-Bernal S, Li K, Neymotin S, Francis J, Principe J and Lytton W 2016 *Frontiers in Neuroscience* **10** 28 ISSN 1662-453X URL https://www.frontiersin.org/article/10.3389/fnins.2016.00028

9. Supplement

9.1. EN/CPN Interleaving

We train a CPN until an EN expires. At that point we train a new EN. Expiration occurs when one of a number of predicates are true:

- The EN prediction loss is greater than $min(6e^{-4}, L/10)$, where L is the most recent task loss. EN prediction loss is an MSE loss between the EN's prediction of muscle trajectories, and the actual muscle trajectories output by the mRNN.
- Task loss increased across 15 of the most previous 30 training epochs.
- 100 CPN training epochs have elapsed.

9.2. Sensor drift

To simulate sensor drift, we add a vector to a bias term introduced to the observation function. We draw the elements of the vector from a mean-0 Gaussian distribution, with variance based on the mean value of the observation function from prior connection-lesion experiments. That allows us to put it into a reasonable range, where it is effective but not extreme. We attempted the experiment with several values of the variance, and found the results to be principally the same: the co-processor eventually learned, but at a rate slower than otherwise. We present results for a variance of $1.5e^{-3}$, which is 2% of the mean observation value.

9.3. Results detail

Experiment	**Lesioned loss**	**Min task loss**	**Min task val loss**	**Pct recov**	**Pct recov val**
AIP No-coadapt	0.004507	0.004599	0.004658	-2.32%	-3.82%
AIP Coadapt	0.004507	0.001575	0.001502	74.41%	76.26%
M1 No-coadapt	0.021136	0.005765	0.005604	74.73%	75.51%
M1 Coadapt	0.021136	0.004772	0.004815	79.55%	79.35%
Con No-coadapt	0.020719	0.002584	0.002583	89.99%	89.99%
Con Coadapt	0.020719	0.002583	0.002405	89.99%	90.88%
Pre-recovery*	0.003834	0.003105	0.003077	22.31%	23.16%
Sensor drift	0.020719	0.002966	0.002825	88.10%	88.83%

Table 1: Losses and recovery. *Pre-recovery lesioned loss and percent recoveries based on the post-recovery values.